Mon. Not. R. Astron. Soc. **000**, 1–6 (2010) Printed 2 February 2011 (MN LaTeX style file v2.2)

Dark Matter in Dwarf Spheroidals

Pascal S. P. Steger[1⋆], Aaron Boley[2], Justin I. Read[1]
[1]*Department of Physics, ETH Zürich, CH-8093 Zürich, Switzerland*
[2]*Department of Astronomy; University of Florida, 211 Bryant Space Science Center, Gainesville, FL 32611, USA*

2 February 2011

ABSTRACT
TODO: check

The dark matter distribution in dwarf galaxies expected from simulations can then be compared with observations, allowing to check the underlying cosmological model. When the typical distribution is known, direct detection dark matter searches can be focused on the densest areas, allowing for a higher annihilation detection rate.

Key words: cosmology: theory, large-scale structure of Universe – galaxies: dwarf spheroidals, evolution – methods: numerical

1 INTRODUCTION

TODO: overview What is Dark Matter? Where is it? How does it influence the buildup of structures like the Milky Way? These are simple questions that seem to need a sophisticated way to find an answer.

1.1 General Background

1.1.1 Dynamics

TODO: intro lecture notes, get basic quantities **?**

TODO: An introduction to dynamics of bound systems is given in e.g. **?**.

1.1.2 Cosmological Models

TODO: intro Weinberg **?** principles of physical cosmology are handled in: **?** the constraints from 5 year WMAP can be found in (Komatsu et al. 2009)

1.1.3 Structure Formation

A review of how we think structure formed through the history of the universe is found in **?**

1.2 Dark Matter

TODO: overview

1.2.1 Evidence for Dark Matter

TODO: formulation

TODO: (Jungman et al. 1996) * rotation curves of galaxies * velocity dispersion in clusters of galaxies * bullet cluster **?** shows that dark matter is indeed particle rather than an effect from alternative gravity

1.2.2 Models

TODO: overview TODO: references * MACHOs * WIMPs * HDM, WDM, CDM, LCDM Hot dark matter (HDM) consists of a particle type that is still freely streaming, as are the neutrinos. Cold dark matter has decoupled from the temperature field in the early universe and started to form small structures, which merge into bigger ones. Warm dark matter is in between these two extremes.

1.2.3 Possibilities for Detection

TODO: references Experiments to detect dark matter directly are described in (**?**). One generally differs between direct and indirect detection: * direct: - annihilation signal from high-energetic particles generated during smash - interaction with detector material needed - sensitive detectors, needs shielding from cosmic rays and radioactive materials * indirect - dynamics - lensing -

To actually detect dark matter, one is interested in the expected density distribution of dark matter in galaxies, as (Navarro et al. 1996) shows.

1.3 Dwarf Galaxies

TODO: Dwarf galaxies represent the smallest observable scales today and are of interest since TODO (Ostriker & Steinhardt 2003). Let us adhere to the definition of dwarf galaxies as the smallest galaxies in the Universe, with dynamical masses $10^6 M_\odot - 10^8 M_\odot$

⋆ E-mail: psteger@phys.ethz.ch

determined from visible components, while star masses range from $\sim 1000 M_\odot$ to $10^7 M_\odot$, and almost no gas is visible.

TODO: overview is given in (Mateo 1998). Star formation histories of the dwarfs is covered e.g. in (Skillman 2005) and (Dolphin et al. 2005), kinematics in (Walker et al. 2009) and (Simon & Geha 2007), and their orbits in (Lux et al. 2010).

1.3.1 Defining Properties

TODO: ref least massive galaxies in universe, mass: TODO

1.3.2 Observations

TODO: all Observations show only of order 100 dwarfs in the Milky Way halo, although there should be thousands of them. This discrepancy is generally known as the "missing satellites problem", (Moore et al. 1999), (Klypin et al. 1999). Recently, wide area surveys discovered more and more dwarfs, (Belokurov et al. 2007), (Belokurov et al. 2009), (Belokurov et al. 2010).

Cusp-Core problem: Observations show a core in the central parts of rotationally supported dwarf galaxies, which is in contrast to theory predicting cuspy profiles for dark matter only profiles, (Moore 1994), (Flores & Primack 1994), (Moore et al. 1999).

Looking at simulated galaxies that are not necessarily rotationally supported, additional constraints as to which properties distinguish cores and cusps can be found. Baryons do play an non-neglectible role in dwarf dynamics, generating cores from cusps via either non-adiabatic contraction or recurring baryonic in-/outflow (Read & Gilmore 2005), which could render the cusp-core problem pointless. This is in fact seen in simulations (Mashchenko et al. 2008), (Governato et al. 2009), which shows that early assumptions on only small influences were wrong (Navarro et al. 1996), (Gnedin & Zhao 2002).

1.4 Globular Clusters

TODO: all Massive star clusters in the halo of the Milky Way - of which some 150 are detected by now **?** - show a mass in stars that is comparable to the dwarf spheroidals, typically 10^5 to $10^6 M_\odot$. The resemblance is going further as they have a similar age; they are mostly old, as old as the Universe itself **?**. The big difference lies in the fact that they show little to no evidence for dark matter in them, whereas dynamics of dwarf spheroidals implies a mass fraction of 90% in dark matter.

Observations of globular clusters in our Galaxy are given in (Zinn 1985) and (De Angeli et al. 2005).

Why should stars form in environments with such a wide spread in density? Is there a connection between dwarf spheroidals and globular star clusters? What is it? It has been proposed **?** that one is the evolved form of the other; or **?** that they form in different environments.

By extracting basic properties that differ in between globular star clusters and dwarf spheroidals, one can try to answer that question. The temporal evolution of the defined substructures gives hints as to whether they represent different phases in an evolutionary path.

The density of globular clusters is such that in a typical patch of the LCDM Universe of size $1\mathrm{Mpc}$ at $z = 10$ contains a few of them (Boley et al. 2009).

1.5 Simulations

TODO: overview The general paradigm behind simulations is as follows:

Take observations of todays structures and try to recover them. This is done via setup of initial conditions similar to the ones that one can see in the cosmic microwave background. There are two different approaches, one assuming gaussianity, the other a little correction term f_{NL}.

These initial conditions are power spectra for the modes of displacement in density and velocity, modeled on a grid of N^3 particles in a box. The box is assumed to repeat itself in each cartesian coordinate, effectively forming a hypertorus.

The simulation is then started and begins to calculate

- gravitational forces between particles
- hydrodynamical quantities, either for hydro particles or on a mesh
- the resulting changes for the next step

TODO: A review of how structure formation can be modeled by numerical means is found in (Bagla 2005)

1.5.1 Ideas

TODO: all

1.5.2 Scopes

TODO: all

1.5.3 Paradigmas

TODO: all *P3M Particle-Particle-Particle-Mesh uses direct summation of forces between all (star/dark matter) particles. *PM *SPH Smoothed particle hydrodynamics approaches the fluids by particles representing volume elements, and calculates the hydrodynamical forces from a discrete form of the Euler equations. *AMR Adaptive mesh refinement describes an advanced technology to follow the liquid more accurately: The mesh is refined in the vicinity of high overdensity, allowing for correct capture of accretion, shock waves, and other small features.

1.5.4 codes

TODO: overview, references *GADGET GADGET is a SPH code. Two versions: Gadget 2 Gadget 3 - TODO: changelog *RAMSES

RAMSES (**?**) uses adaptive mesh refinement technique to handle hydrodynamic properties. Its hydrodynamical solver involves a second order Godunov scheme.

*ENZO, GASOLINE,...

1.6 Overview this work

1.6.1 TOC

This work is organized in the following way: After this introduction with an overview over the widespread field of dark matter research and methods of numerics in cosmology, we start by describing the simulations performed in section 2, followed by a short explanation on the methods in section 3. Then we focus on results: section 4 first concentrates on halo finding performance and general properties of the halos in the high resolution, hydrodynamical run, both for dark

Figure 1. Visualization by ray-tracing of one of the dwarf spheroidals in the high resolution hydro run. The visible box size spans a range of $TODO\,\mathrm{Mpc}/h$.

matter/stars and gas. This is compared with the properties found in the dark matter only run, allowing to draw conclusions on the influence of baryons.

1.6.2 Novelties

TODO: all

2 THE DATA

TODO: overview

2.1 The Simulations

TODO: overview Three simulations were run for this project. The main simulation was run with high resolution with nonequilibrium physics. For comparative reasons the same resolution was used for a dark matter only simulation, and convergence was investigated by a comparing that one to a lower dark matter only simulation. All simulations used the same cosmology, as follows.

2.1.1 Cosmological Parameters

TODO: all, acc. ref

The high resolution hydrodynamical simulation was run with WMAP-5 concordance cosmology parameters, i.e. $\Omega_\Lambda =$, $\Omega_M =$, $\Omega_b =$, $h =$, $\sigma_8 =$

2.1.2 Initial Conditions

TODO: all

Initial conditions were generated with GRAFIC, for a box of $1\mathrm{Mpc}/h$ boxlength, at $z =$, with a low resolution boundary layer of 128^3 equivalent particles and an inner high resolution region of 256^3 particles. The dark matter only, high resolution run was performed with 512^3 particles.

Simulation	$M_{\rm vir}/h^{-1}\mathrm{M}_\odot$	$R_{\rm vir}/h^{-1}\mathrm{Mpc}$	$N_{\rm sub}$	$N_{\rm field}$
s1	2.8900×10^{14}	1.3466	502	218
s2	1.6021×10^{14}	1.1062	279	200
s3	2.4922×10^{14}	1.2817	399	163

Table 1. Properties of the five most massive halos. $M_{\rm vir}$ and $R_{\rm vir}$ are the virial mass and radius of the halos.

2.1.3 Stepping, motivation for stop @ z=10

TODO: all

It has been shown in (**?**) that in a typical volume of $1\mathrm{Mpc}/h$ at $z \sim 10$ there should be a few dwarf spheroidal galaxies present. In short, this can be calculated via TODO: derivation

2.1.4 UV background, ram pressure

TODO: all

2.1.5 SN feedback

TODO: all

2.1.6 Black Holes

TODO: all Active galactic nuclei emit energy during accretion of material, which is fed back into the surroundings. The main effect is

2.2 Higher Resolution

TODO: all

We use significantly higher resolution than was previously performed (Boley et al. 2009), with non-equilibrium physics included (Abel et al. 1997).

The force resolution (Plummer's equivalent length) in the highest resolution mesh is $4pc/h$ at $z = 10$, which sets a restriction on the determination of densities in the inner regions of the smallest halos. It is indicated as a vertical line in the graphs of radial profiles.

TODO: update table

3 METHODS

TODO: ov

3.1 Definitions

TODO: all

* spherical overdensity *

3.2 Halo Finding

TODO: all

The simulation outcome by itself shows only properties of individual dark matter particles, and additionally a mesh for the hydrodynamical constituents. One is interested in bound substructures, which have to be found first. To do so, a halo finder needs to be invoked.

* FOF The friend-of-friends algorithm as e.g. described in (**?**) starts with a particle and searches for its nearest neighbor. After doing this iteratively, all particles connected by such a chain are considered to lie within the same halo. This procedure works well for isolated halos only. (TODO: check)

* HOP HOP from the RAMSES toolkit starts off pretty much the same way, but only allowing particles at positions of smaller potential energy as neighbors. All particles ending on the same particle are then assigned the same halo.

* watershed The watershed algorithm (**?**) starts from the density maxima as leaves of the halo/subhalo tree. Stepping further out, all material in the same potential pot is assigned to the respective maxima. As soon as a neighbor maximum is encountered, both halos form an additional leave in the tree.

* SOD The spherical overdensity algorithm as provided by RAMSES (TODO: does what). It does not handle correctly the cases of mergers, yielding a halo position in the middle of both merging halos.

Here the AHFSTEP algorithm of the simulation code AMIGA is used. It showed superior capabilities with mock halos and subhalos (**?**). The Ramses simulation snapshots are first converted to Gadget format, allowing a simple read-in for AHFSTEP.

The prospective halo centers can be defined in several ways: by the position of the center of mass, by the position of the most bound particle, by density maxima or TODO. We got best results with TODO. (TODO: checked it visually). An additional iterative procedure excludes all particles which are kinematically unbound: if the kinetic and internal energy (for hydro particles) exceed the potential energy, the particle is removed, the potential recalculated and further unbound particles excluded. A mean fraction of TODO

TODO: for high mass/low mass systems

AHFSTEP outputs a bunch of quantities, for the next steps only position and virial radius (inside which $\Delta\rho = 200$) are used.

Additional displacements with respect to the densest point are corrected with an additional shrinking sphere algorithm: It start from the center of mass of all particles in a sphere of $3r_{\rm vir}$ radius, then subtracts a fixed distance from the radius, and considers only particles inside the smaller sphere to find the center of mass in the next step. Displacement up to TODO have been measured this way, owing to the fact that spherical symmetry is rarely given.

TODO: fractional change!!

All particles in a sphere around the halo centers

4 RESULTS

TODO: ov

4.1 Halo finding

4.2 DM density profile

TODO: all

method:

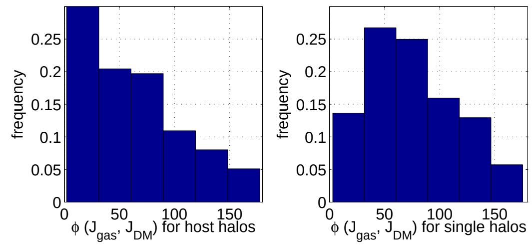

Figure 2. Positions of the halos detected by SOD (blue circle) and AHF (red crosses) on top of dark matter density

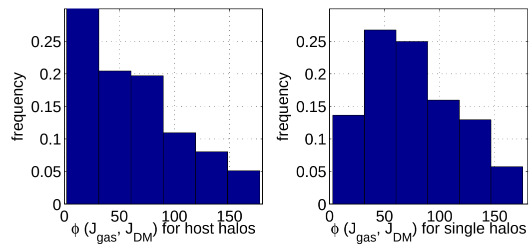

Figure 3. Positions of the halos detected by SOD (blue circles) and AHF (red crosses) on top of gas density

4.3 Gas Density Profile

TODO: all

4.4 Temporal Evolution

TODO: all The simulation produced output snapshots in regular intervals, allowing for an investigation on how the different values change with epoch.

5 SUMMARY AND DISCUSSION

TODO: overview

5.1 Impacts on Formation History

TODO: all

5.2 Further Evolution down to z=0

TODO: all

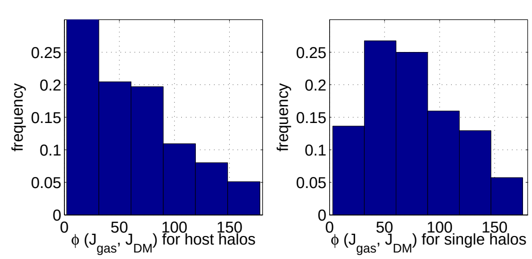

Figure 4. Distribution of additional position correction by shrinking sphere algorithm.

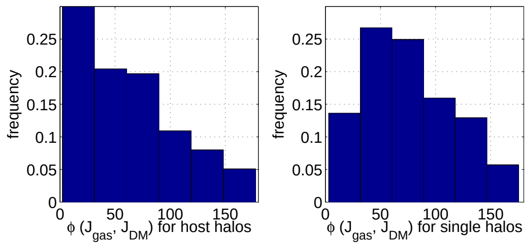

Figure 5. Dark matter density profile of the five most massive halos

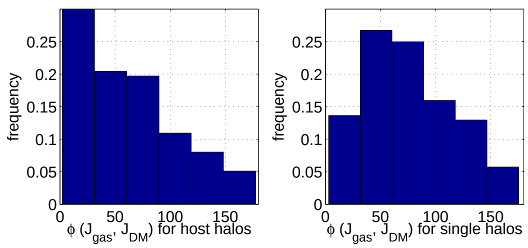

Figure 6. Core radius versus mass for all halos.

5.3 Local DM Density

TODO: all

ACKNOWLEDGEMENTS

TODO: Read, Boley, Garbari, Hobbs, Teyssier S. Garbari provided a prototype algorithm for the correction of the prospective halo centers. A. Boley gave numerous hints of technical nature, and provided sample scripts for starting analysis.

6 APPENDIX: NUMERICAL ROBUSTNESS, CONVERGENCE

The low resolution simulation was used to check convergence of the high resolution dark matter only simulation.

REFERENCES

Abel T., Anninos P., Zhang Y., Norman M. L., 1997, Nature, 2, 181
Bagla J. S., 2005, Current Science, 88, 1088

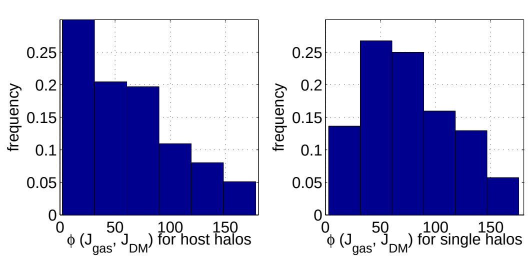

Figure 7. Distribution of slopes for core and outskirt

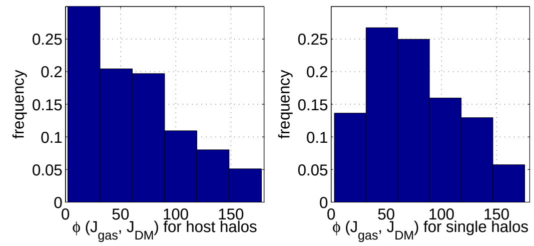

Figure 8. Density profile of star particles in the five most massive halos

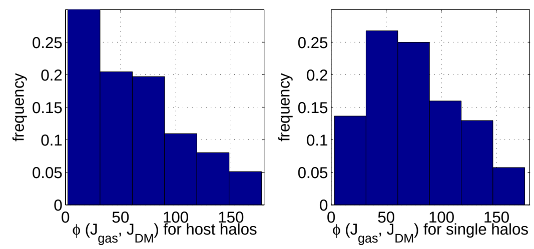

Figure 9. Fraction of stellar mass to dark matter mass in all halos with $M < TODO$

Belokurov V., Walker M. G., Evans N. W., Gilmore G., Irwin M. J., Just D., Koposov S., Mateo M., Olszewski E., Watkins L., Wyrzykowski L., 2010, ApJ, 712, L103
Belokurov V., Walker M. G., Evans N. W., Gilmore G., Irwin M. J., Mateo M., Mayer L., Olszewski E., Bechtold J., Pickering T., 2009, MNRAS, 397, 1748
Belokurov V., Zucker D. B., Evans N. W., Kleyna J. T., Koposov S., Hodgkin S. T., Irwin M. J., Gilmore G., Wilkinson M. I., Fellhauer M., Bramich D. M., 2007, ApJ, 654, 897
Boley A. C., Lake G., Read J., Teyssier R., 2009, ApJ, 706, L192
De Angeli F., Piotto G., Cassisi S., Busso G., Recio-Blanco A., Salaris M., Aparicio A., Rosenberg A., 2005, AJ, 130, 116
Dolphin A. E., Weisz D. R., Skillman E. D., Holtzman J. A., 2005, ArXiv Astrophysics e-prints
Flores R. A., Primack J. R., 1994, ApJ, 427, L1
Gnedin O. Y., Zhao H., 2002, MNRAS, 333, 299
Governato F., Brook C., Mayer L., Brooks A., Rhee G., Wadsley J., Jonsson P., Willman B., Stinson G., Quinn T., Madau P., 2009, ArXiv e-prints
Jungman G., Kamionkowski M., Griest K., 1996, Phys. Rep., 267, 195
Klypin A., Kravtsov A. V., Valenzuela O., Prada F., 1999, ApJ, 522, 82

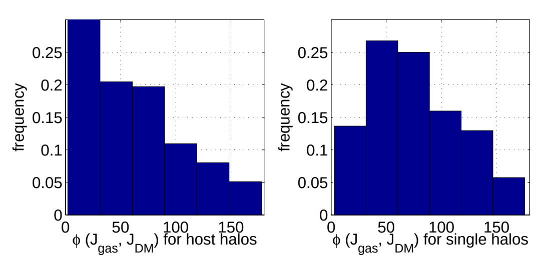

Figure 10. Density profile of gas in the five most massive halos

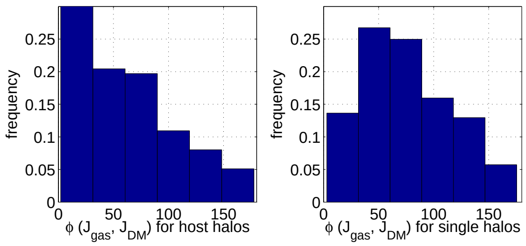

Figure 11. Radial dependence of star metallicities for $metal > metal_*$ and $metal < metal_*$

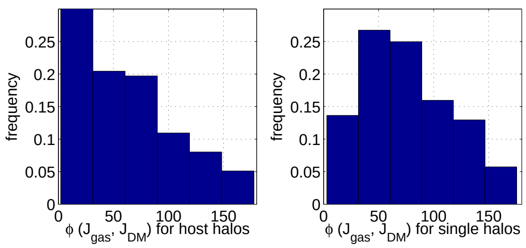

Figure 12. Core radius as a function of time, for the five most massive halos

Komatsu E., Dunkley J., Nolta M. R., Bennett C. L., Gold B., Hinshaw G., Jarosik N., Larson D., Limon M., Page L., Spergel D. N., Halpern M., Hill R. S., Kogut A., Meyer S. S., Tucker G. S., Weiland J. L., Wollack E., Wright E. L., 2009, ApJS, 180, 330
Lux H., Read J. I., Lake G., 2010, MNRAS, 406, 2312
Mashchenko S., Wadsley J., Couchman H. M. P., 2008, Science, 319, 174
Mateo M. L., 1998, ARA&A, 36, 435
Moore B., 1994, Nature, 370, 629
Moore B., Ghigna S., Governato F., Lake G., Quinn T., Stadel J., Tozzi P., 1999, ApJ, 524, L19
Moore B., Quinn T., Governato F., Stadel J., Lake G., 1999, MNRAS, 310, 1147
Navarro J. F., Frenk C. S., White S. D. M., 1996, ApJ, 462, 563
Ostriker J. P., Steinhardt P., 2003, Science, 300, 1909
Read J. I., Gilmore G., 2005, MNRAS, 356, 107
Simon J. D., Geha M., 2007, ApJ, 670, 313
Skillman E. D., 2005, Nature, 49, 453
Walker M. G., Mateo M., Olszewski E. W., Peñarrubia J., Wyn Evans N., Gilmore G., 2009, ApJ, 704, 1274
Zinn R., 1985, ApJ, 293, 424

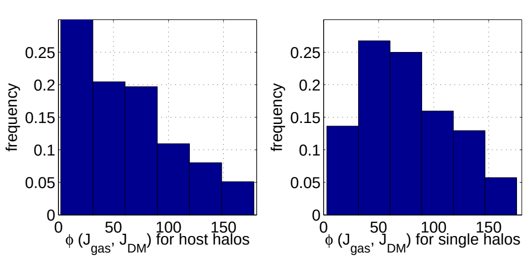

Figure 13. Correlation between core radii detected in low resolution (abscissa) and high resolution run (ordinate).

all references from reading list +both Oh2010